Influence of Boron doping on microcrystalline silicon growth*

Li Xin-Li(李新利)[a], Chen Yong-Sheng(陈永生)[a], Yang Shi-E(杨仕娥)[a], Gu Jin-Hua(谷锦华)[a], Lu Jing-Xiao(卢景霄)[a]†, Gao Xiao-Yong(郜小勇)[a], Li Rui(李 瑞)[a][b], Jiao Yue-Chao(焦岳超)[a], Gao Hai-Bo(高海波)[a], and Wang Guo(王 果)[a]

[a] *The Key Laboratory of Material Physics of Ministry of Education, School of Physics and Engineering, Zhengzhou University, Zhengzhou* 450052, *China*

[b] *Henan University of Technology, Zhengzhou* 450051, *China*

(Received 28 December 2010; revised manuscript received 18 May 2011)

Microcrystalline silicon (μc-Si:H) thin films with and without boron doping are deposited using the radio-frequency plasma-enhanced chemical vapour deposition method. The surface roughness evolutions of the silicon thin films are investigated using ex situ spectroscopic ellipsometry and an atomic force microscope. It is shown that the growth exponent β and the roughness exponent α are about 0.369 and 0.95 for the undoped thin film, respectively. Whereas, for the boron-doped μc-Si:H thin film, β increases to 0.534 and α decreases to 0.46 due to the shadowing effect.

Keywords: microcrystalline silicon thin film, surface roughness, shadowing effect

PACS: 68.55.ag, 68.55.jm, 68.37.Ps **DOI:** 10.1088/1674-1056/20/9/096801

1. Introduction

Microcrystalline silicon (μc-Si:H) films[1−3] have been a subject of extensive studies because of their importance in device applications.[4] The boron-doped μc-Si:H in a μc-Si:H solar cell plays the roles of seed, window layer and forms a junction. Its properties are crucial in obtaining high efficiency solar cells. As a fast, non-destructive and precise optical tool, spectroscopic ellipsometry (SE)[5−8] has been used to study the growth mechanism of the μc-Si:H film, for example, Kurmar *et al.*[9] studied a-Si:H and μc-Si:H films obtained by glow discharge deposition using SE. Kohd *et al.*[10] studied the effect of different boron dopant source gases on the nucleation and growth of p-type μc-Si:H film using real-time SE. Gu *et al.*[11] analysed the growth model of the μc-Si:H film deposited with the very high frequency plasma-enhanced chemical vapor deposition (VHF-PECVD) method using ex situ SE. However, the growth mechanism of the boron-doped μc-Si:H has been less analysed using SE.

In this paper, ex situ SE, atomic force microscopy (AFM) and Raman spectroscopy are used to study the structural characteristics of doped and undoped μc-Si:H thin films. A comparison between the SE and the AFM measurements of the μc-Si:H thin film surface roughness is made to reveal the growth mechanism of the p-type μc-Si:H film.

2. Experimental details

μc-Si:H thin films with and without boron doping were deposited on glass substrates using a conventional capacitive coupled radio-frequency plasma-enhanced chemical vapor deposition (RF-PECVD) system. The deposition parameters were as follows. The total gas flow was 200 sccm,[12] the distance between two electrodes was fixed at 2.5 cm, and the plasma power and the deposition pressure were 150 W and 266 Pa, respectively. The silane and diborane concentrations are defined as[13] $C_{\rm Si} = F_{\rm SiH_4}/(F_{\rm H2} + F_{\rm SiH_4})$ and $C_{\rm B} = F_{\rm B_2H_6}/F_{\rm SiH_4}$, respectively, where $F_{\rm SiH_4}$, $F_{\rm H_2}$ and $F_{\rm B_2H_6}$ represent the flow rates of SiH_4, H_2 and B_2H_6, respectively. Two series of undoped thin films were prepared. Series A was deposited at

*Project supported by the National Key Basic Research Program of China (Grant No. 2011CB201606) and the National Natural Science Foundation of China (Grant No. 51007082).

†Corresponding author. E-mail: jxlu@zzu.edu.cn

© 2011 Chinese Physical Society and IOP Publishing Ltd

a substrate temperature of 150 °C and $C_{Si} = 1\%$, while series B was deposited at a substrate temperature of 180 °C and $C_{Si} = 1.5\%$. For the boron-doped thin films, the substrate temperature was 180 °C, $C_{Si} = 1.5\%$ and $C_B = 0.4\%$.

After the deposition, the SE parameters sensitive to surface properties were measured in time by SE. The incident angle was fixed at 70°. The optical spectra in the range from 200 nm to 1000 nm were measured in steps of 10 nm. The SE parameters ψ and Δ were fitted by using WVASE32 software. The surface morphologies and the root-mean-square (RMS) roughness of the boron-doped μc-Si:H thin films were taken over an area of 2 μm × 2 μm using an atomic force microscope (SHIMADZU SPM-9500 J3) in contact mode. The film crystallinity was characterized by Raman spectroscopy using a Renishaw 2000 Raman spectrometer with 632.8 nm laser excitation. The output power was 5.32 mW.

3. Results and discussion

Figure 1 shows the AFM surface images of the boron-doped μc-Si:H thin films with different film thicknesses. With progressive growth of the film, smaller grains tend to cohere with their adjoining ones, i.e., start to conglomerate and grow upward and laterally, acquiring a columnar shape.[14] The grains and their conglomerates exhibit different shapes and different sizes with the film growth.

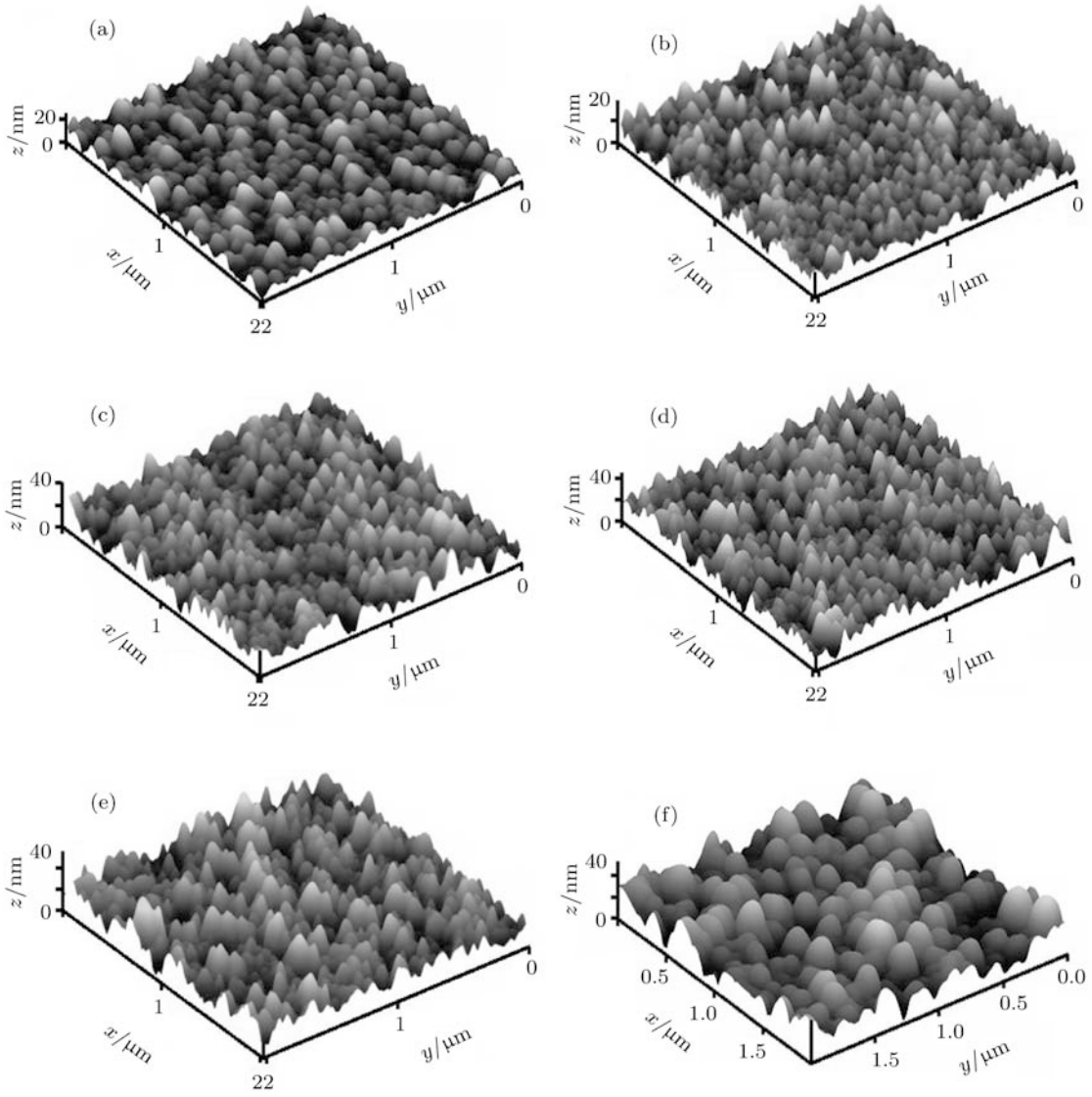


Fig. 1. AFM surface morphologies of boron-doped μc-Si:H thin films with different film thicknesses: (a)112 nm, (b)145 nm, (c) 190 nm, (d) 223 nm, (e) 274 nm and (f) 309 nm.

Figure 2 shows the SE spectra of boron-doped μc-Si:H thin films with different film thicknesses. The number of wave hollows increases with the increase of the thickness of the film. The change of parameters ψ and Δ shows the film structural transformation. The structural characteristics can be obtained from SE spectra fitting.

Figures 3(a) and 3(b) show the measured dispersion relations of the imaginary components of pseudo-dielectric function $\langle\varepsilon_2\rangle$ for the undoped and the boron-doped μc-Si:H thin films with different deposition times, respectively. The dielectric function ε_2 for the films shows strong shoulders near E_1 (∼3.5 eV) and E_2 (∼4.2 eV), revealing a crystalline structure. These peaks are related to the critical points in the joint density of states of the single crystal silicon and are very sensitive to the size and volume of the crystallites. In general, the $\langle\varepsilon_2\rangle$ spectra include data on the film thickness, the bulk optical constants and the surface roughness.[15] The amplitude of $\langle\varepsilon_2\rangle$ in the high energy part of the spectra continuously decreases, which is accompanied with a red-shift as the deposition time increases. This is a characteristic of an increase of surface roughness.[16,17]

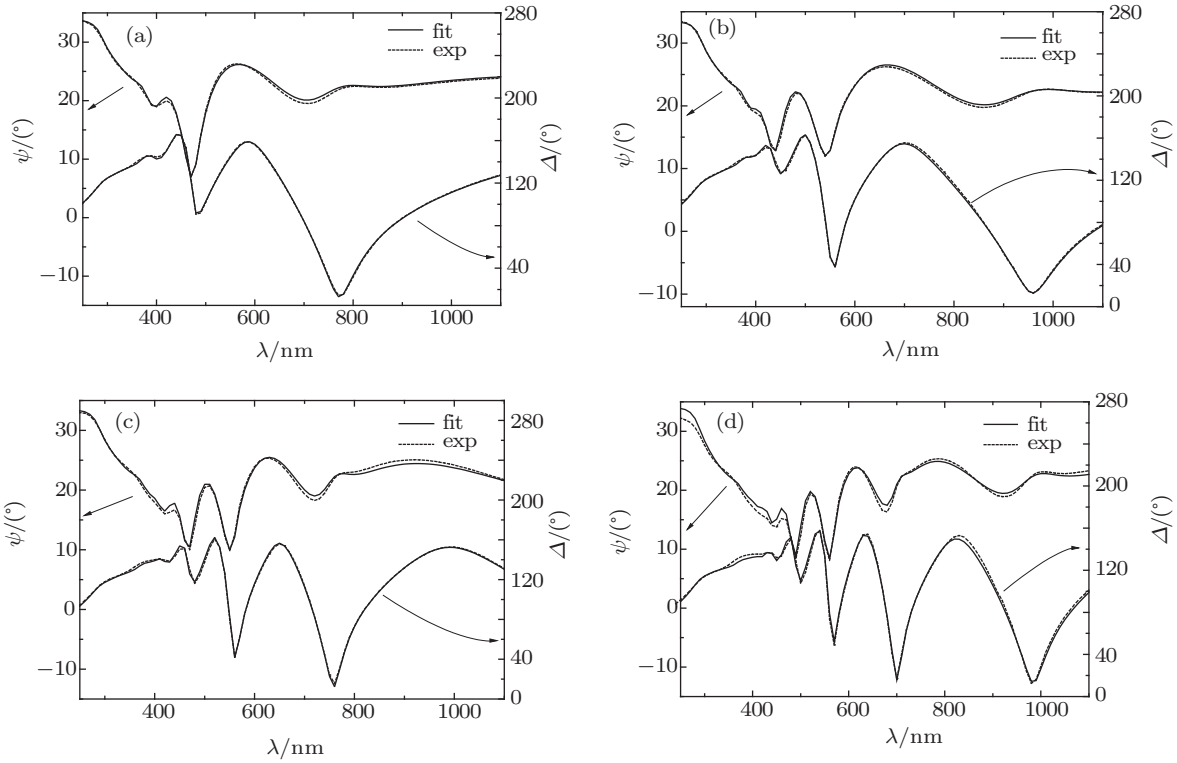


Fig. 2. SE spectra of boron-doped μc-Si:H films with different thicknesses: (a) 112 nm, (b) 145 nm, (c) 223 nm and (d) 309 nm. The dashed lines denote the fit spectra using the three-layer model.

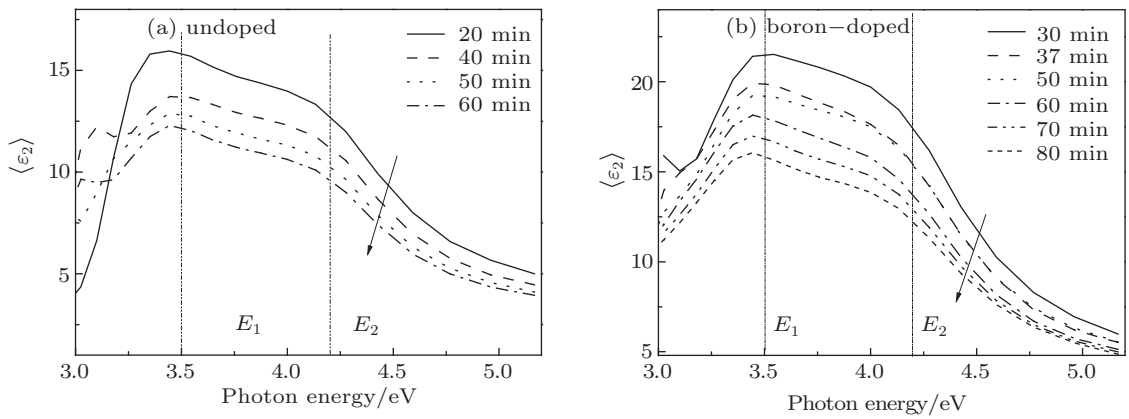


Fig. 3. Evolutions of the imaginary components of the pseudo-dielectric function $\langle\varepsilon_2\rangle$ for (a) undoped and (b) boron-doped μc-Si:H thin films with different deposition times.

According to the KPZ model,[18,19] film surface roughness d_s and film thickness d satisfy the relation $d_s \sim d^{\beta}$, where β is the growth exponent related to the film growth mechanism.[20] The $\beta = 1/2$, $1/3$ and 0 denote the processes of zero diffusion limited random growth, finite diffusion growth and step flow growth, respectively. The surface roughness varies with the film thickness.

Figure 4 shows the RMS roughness measured by AFM (σ_{rms}) and the top surface layer thickness d_s deduced from the SE fittings. The roughness measured by SE is higher, while that measured by AFM is lower for the same sample. The deviation is attributed to the different measurement mechanisms. The relationship between d_s and σ_{rms} found in our case is similar to that observed by Sanjay *et al.*[14] and Fujiwara *et al.*[21] Therefore, the possibility of the SE method to accurately calculate the thickness and the surface roughness of the film is demonstrated.

The log–log plots of the surface roughness and layer thickness d_s versus film thickness d are shown in Fig. 4. In the case of the undoped μc-Si:H films deposited at 150 °C, the value of $\beta = 0.395$ is close to 1/3, namely, the limited diffusion model, and β decreases to 0.369 with the deposition temperature increasing to 180 °C. The decrease of β indicates the enhanced diffusion of the precursors on the surface attributable to the increase of the surface temperature. A similar roughness increase is observed in the μc-Si:H growth on a Si (111) substrate at temperatures around 150–200 °C.[22] However, for the boron-doped thin films deposited at 180 °C, β increases rapidly to 0.534, which is larger than 0.5 for the zero diffusion limited random growth in scaling theory.

Raman spectroscopy is a useful tool to study the crystallinity (X_c) of thin films, $X_c = (I_{510} + I_{520})/(I_{480} + I_{510} + I_{520})$,[23] where I_{520} and I_{510} are the intensities of the crystalline-like peaks, whereas I_{480} is the intensity of the amorphous-like peak due to the transverse optic Si–Si vibration in the Raman spectra. Figures 4(a) and 4(d) show the dependence of the X_c on the thickness of the doped and the undoped films, respectively. For the undoped films, the X_c increases rapidly with the film thickness increasing from 52 nm to 162 nm. For the doped thin films, the X_c increases rapidly then slightly and becomes saturated, as the thickness changes from 112 nm to 309 nm. It can be seen that the films deposited under different conditions are both crystallized and the X_c increases with the increase of the thin film thickness. Increasing the thin film thickness will result in an increase of the size of the grain.

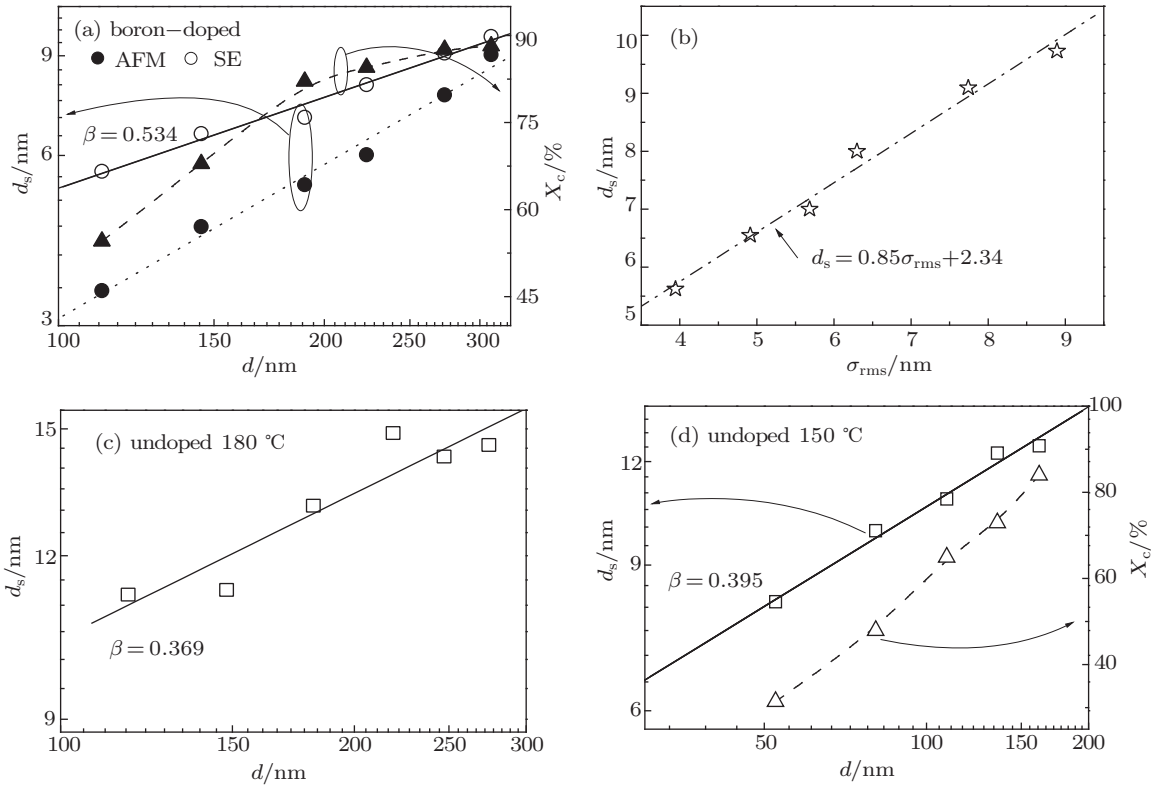


Fig. 4. Variations of surface roughness layer thickness and X_c with the film thickness for (a) boron-doped and (c) undoped μc-Si:H thin films deposited at 180 °C and (d) undoped μc-Si:H thin films deposited at 150 °C. (b) Correlation between RMS and d_s for the boron-doped films.

The quantitative information about the surface morphology can be obtained from the height–height correlation function $H(r)$ defined as[24,25]

$$H(r) = \left\langle [h(r) - h(0)]^2 \right\rangle \sim \begin{cases} r^{2\alpha}, & r \ll \zeta, \\ 2w^2, & r \gg \zeta, \end{cases}$$

where r is the position in the plane perpendicular to the growing direction, $h(r)$ is the surface height at position r, bracket $\langle\ \rangle$ denotes the spatial and ensemble average, α is the roughness exponent related to the short-range regime and describes how 'wiggly' the local slope is, ζ is the lateral correlation length and w is the RMS surface roughness. Figure 5 shows the $H(r)$ curves for the undoped and the boron doped thin films, each as a function of the distance. The $H(r)$ is calculated from the AFM images for the undoped and the boron-doped films. It is shown that the $H(r)$ curves are not parallel to each other until the deposition time reaches 60 min. However, for the boron-doped thin films, we can see that the $H(r)$ curves are parallel to each other. The α is 0.95 for the undoped μc-Si:H films, while it decreases to 0.46 for the boron-doped ones.

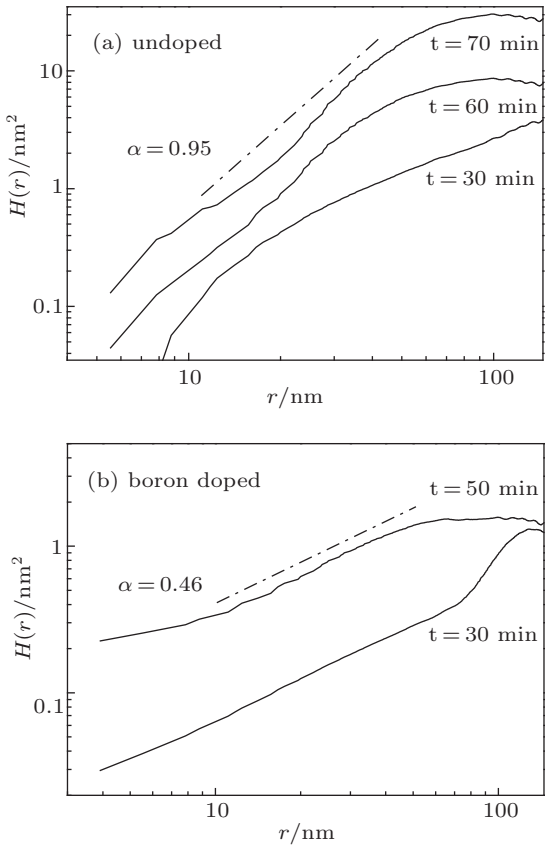


Fig. 5. The $H(r)$ curves for undoped and boron doped thin films, each as a function of r, plotted in log–log scale.

A conventional dynamic scaling approach can always be used to describe the morphological evolution of a growth front. The α and β are two scaling exponents presenting different meanings. α is sensitive to the local surface structure and β is related to the time-dependent long-range surface feature. In theory, a larger value of α corresponds to a locally smoother surface structure and a smaller value of α corresponds to a more jagged local surface morphology. For the boron-doped thin film, β is 0.534, which is larger than 0.5 for the zero diffusion limited random growth in the scaling theory. There are some roughening increasing mechanisms. First, B_2H_6 may have a catalytic effect. B-containing radicals on the substrate surface at the initial stages of the p-layer growth act as catalysts to shift the attaching–detaching equilibrium of the SiH_x precursors toward the attaching direction. As a result, highly dense nuclei have been observed in a short deposition time.[10] We also take into account the shadowing effect, i.e., some surface points are shadowed from the incident flux of particles due to high surface features nearby. The shadowing effect results in the non-uniform distribution of the incident flux on the growing surface. The local low surface receives fewer incoming particles than the high surface. The strength of the shadowing effect is closely related to the sticking coefficient of the precursor, which is the probability of the impinging flux reacting with the substrate.[26] Recently, Pelliccione *et al.*[27] used Monte Carlo simulations and experimental results to show that during the film deposition a mound structure could be formed. The formation of a mound structure is due to a nonlocal growth effect, such as the shadowing, which leads to the breakdown of the self-affinity of the morphology described by the well-established dynamic scaling theory.

The nonlocal effect, such as shadowing, along with the redistribution of the atoms reflected from the surface due to the nonunity sticking coefficient[26] can play an important role in determining surface morphology during the growth. The nonlocal effect gives rise to a mound structure that cannot be described within the context of self-affinity. The primary nonlocal growth effect is the shadowing effect,[28,29] i.e., taller surface features block the incoming flux from reaching lower lying areas of the film. This allows the taller surface features to grow at the expense of the shorter ones, leading to coarsening of the surface. Shadowing is an inherently nonlocal process, because the shadowing of a surface feature depends on the heights of all other surface features, not just close or local ones.[27]

During p-type film growth, the doped boron can promote nucleation and re-nucleation, and can increase the nucleation density, resulting in a change in the growth model. If only the shadowing effect is present, we would expect $\beta = 1$, no matter how small the shadowing effect is.[26] Therefore, there may exist mechanisms other than shadowing and the nonlocal effect. The formation mechanism may be correlated with the surface hydrogen.[22] The growth mechanism of the boron-doped Si thin film needs to be further studied.

4. Conclusion

Microcrystalline silicon (μc-Si:H) thin films with and without boron doping are deposited using the RF-PECVD method. The surface roughness evolution of the silicon thin film is investigated using ex situ SE and AFM. A high degree of correlation exists between the two measurements. Based on the KPZ model, the growth behaviour of the μc-Si:H thin film is studied. The growth exponent β and the roughness exponent α are 0.369 and 0.95 for the undoped thin film deposited at a substrate temperature of 180 °C, respectively. The β value corresponds to the limited diffusion model. The growth exponent β increases with the decrease of the deposition temperature. However, for the boron-doped μc-Si:H thin film, β increases to 0.534, and α decreases to 0.46. To some extent, the formation mechanism is correlated with the shadowing effect and the nonlocal effect. Due to the boron catalysis effect, the reaction radical BH_x aggregation is promoted, which results in the shadowing effect.

References

[1] Li T W, Liu F C and Zhu M F 2011 *Acta Phys. Sin.* **60** 18103 (in Chinese)

[2] Chen Y S, Xu Y H, Gu J H, Lu J X, Yang S E and Gao X Y 2010 *Chin. Phys.* B **19** 087206

[3] Chen Y S, Yang S E, Wang J H, Lu J X, Gao X Y and Gu J H 2010 *Chin. Phys.* B **19** 057205

[4] Yang S E, Wen L W, Chen Y S, Wang C Z, Gu J H, Gao X Y and Lu J X 2008 *Acta Phys. Sin.* **57** 5176 (in Chinese)

[5] Liu M X, Li B C, Gao W D and Han Y L 2010 *Acta Phys. Sin.* **59** 1632 (in Chinese)

[6] Zhang J T, Li Y and Luo Z Y 2010 *Acta Phys. Sin.* **59** 0186 (in Chinese)

[7] Zhou Y, Wu G S, Dai W, Li H W and Wang A Y 2010 *Acta Phys. Sin.* **59** 2356 (in Chinese)

[8] Gao X Y, Feng H L, Ma J M and Zhang Z Y 2010 *Chin. Phys.* B **19** 090701

[9] Kumar S, Pandya D K and Chopra K L 1988 *J. Appl. Phys.* **63** 1497

[10] Koh J, Fujiwara H, Koval R J, Wronski C R and Collins R W 1999 *J. Appl. Phys.* **85** 4141

[11] Gu J H, Ding Y L, Yang S E, Gao X Y, Chen Y S and Lu J X 2009 *Acta Phys. Sin.* **58** 4123 (in Chinese)

[12] Hadjaj A, Pham N, Cabarrocas P R I and Jbara O 2009 *Appl. Phys. Lett.* **94** 061909

[13] Chen Y S, Yang S E, Wang J H, Lu J X, Gao X Y, Gu J H, Zheng W and Zhao S L 2008 *Chin. Phys.* B **17** 1394

[14] Sanjay K R, Satyendra K, Dinesh D and Cabarrocas P R I 2007 *Thin Solid Films* **515** 7619

[15] Jia H J and Shirai H 2006 *Thin Solid Films* **506–507** 27

[16] Kumar S, Drevillon B and Godet C 1986 *J. Appl. Phys.* **60** 1542

[17] Hadjadj A, Pham N, Roca I, Cabarrocas P, Jbara O and Djellouli G 2010 *J. Appl. Phys.* **107** 083509

[18] Kardar M, Parisi G and Zhang Y C 1986 *Phys. Rev. Lett.* **56** 889

[19] Qi H J, Huang L H, Shao J D and Fan Z X 2003 *Acta Phys. Sin.* **52** 2743 (in Chinese)

[20] Zhu Z L, Ding Y L, Wang Z Y, Gu J H and Lu J X 2010 *Chin. Phys.* B **19** 106803

[21] Fujiwara H, Kondo M and Mastuda A 2001 *Phys. Rev.* B **63** 115306

[22] Kondo M, Ohe T, Saito K, Nishimiya T and Mstsuda A 1998 *J. Non-Cryst. Solids* **227–230** 890

[23] Chen Y S, Gao X Y, Yang S E, Lu J X and Gu J H 2007 *Acta Phys. Sin.* **56** 4122 (in Chinese)

[24] Gu J H, Zhou Y Q, Zhu M F, Liu F Z and Liu J L 2005 *J. Non-Cryst. Solids* **285** 491

[25] Karabacak T, Zhao Y P, Wang G C and Lu T M 2001 *Phys. Rev.* B **64** 085323

[26] Zhao Y P, Drotar J T, Wang G C and Lu T M 2001 *Phys. Rev. Lett.* **87** 136102

[27] Pelliccione M, Karabacak T and Lu T M 2006 *Phys. Rev. Lett.* **96** 146105

[28] Tang C, Slexander S and Bruinsma R 1990 *Phys. Rev. Lett.* **64** 772

[29] Yao J H and Guo H 1993 *Phys. Rev.* E **47** 1007